

Mitigating future glacial lake outburst floods in the Himalaya

Xue Wang^{a,b†}, Wenfeng Chen^{a†*}, Guoqing Zhang^{c,a*}, Adam Emmer^{d,e}, Holger Frey^f, Caroline Taylor^g, Christian Hugel^f, Ashim Sattar^h, Guoxiong Zhengⁱ, Irfan Rashidi^j, Jonathan L. Carrivick^k, Georg Veh^l, Simon Allen^{f,m}, Jakob Steiner^{d,n}, Duncan Quincey^k, Martin Mergili^d

^a State Key Laboratory of Tibetan Plateau Earth System, Environment and Resources (TPESER), Institute of Tibetan Plateau Research, Chinese Academy of Sciences, Beijing 100101, China

^b University of Chinese Academy of Sciences, Beijing 100049, China

^c Key Laboratory of Biodiversity and Environment on the Qinghai-Tibetan Plateau, Ministry of Education, School of Ecology and Environment, Xizang University, Lhasa 850000, China

^d Institute of Geography and Regional Science, University of Graz, Graz 8010, Austria

^e Department of Physical Geography and Geoecology, Faculty of Science, Charles University, 128 00 Prague 2, Czechia

^fDepartment of Geography, University of Zurich, Zurich 8057, Switzerland

⁹School of Geography, Politics and Sociology, Newcastle University, Newcastle upon Tyne NE1 7RU, UK

^h School of Earth, Ocean and Climate Sciences, IIT Bhubaneswar, Odisha 752050, India

ⁱCollege of Earth and Environmental Sciences, Lanzhou University, Lanzhou 730000, China

^jDepartment of Geoinformatics, University of Kashmir, Hazratbal Srinagar 190006, India

^k School of Geography and water@leeds, University of Leeds, Leeds LS2 9JT, UK

⁴Institute of Environmental Science and Geography, University of Potsdam, Potsdam-Golm 14476, Germany

^m*Institute for Environmental Sciences, University of Geneva, Geneva CH-1211, Switzerland*

ⁿ Himalaya University Consortium, Lalitpur 44700, Nepal

[†]These authors contributed equally.

*Corresponding author.

Email: guoqing.zhang@itpcas.ac.cn (G.Zhang); chenwf@itpcas.ac.cn (W.Chen)

31 **Abstract**

32 Glacial lake outburst floods (GLOFs) are among the most severe cryospheric hazards in the Himalaya. While
33 previous studies have primarily focused on the characteristics and causes of GLOFs, strategies for mitigating
34 their disaster impacts remain underexplored. This study introduces China's Glacial Lake Management System
35 (GLMS) and evaluates its potential for regional replication in reducing damage caused by GLOFs. We find that
36 while GLOF frequency shows a statistically insignificant decrease from 1990 to 2023, downstream damage has
37 intensified, yet appears relatively mitigated within China across the Himalaya following the implementation
38 of the GLMS. Further hydrodynamic modelling suggests that glacial lakes will continue to expand in the future,
39 with total growth expected to triple relative to the 2000–2020 period. These expansions could increase GLOF
40 exposure by over 27% for high-risk lakes and by more than 40% in regions outside China without targeted
41 interventions. However, implementing GLMS engineering measures could reduce the intensity of future floods
42 by 24%, with even greater reductions outside China—29% compared to 21% within China. Building on China's
43 lake management experience and recognizing the transboundary nature of GLOFs, the comprehensive
44 framework we propose for region-wide glacial lake risk reduction across the Himalaya integrates engineering
45 measures, early warning systems, and community responses. This framework addresses the urgent need for
46 proactive and coordinated mitigation strategies in densely populated high-mountain regions.

47

48 **Keywords:** Himalaya, glacial lake outburst floods (GLOFs), flood intensity, Glacial Lake Management System
49 (GLMS), risk mitigation strategies

51 **1. Introduction**

52 Glacial lake outburst floods (GLOFs) are a significant cryospheric threat in the Himalaya, affecting regions
53 spanning the Hindu Kush, Karakoram, Himalaya, Nyainqêntanglha and Hengduan mountains. These events
54 often cause widespread and catastrophic damage to downstream communities, infrastructure, farmland and
55 ecosystems [1-3]. For example, a recent GLOF event on 8 July 2025 in a China-Nepal transboundary river basin
56 in Gyirong County, Xigazê, Xizang, left 17 people missing and caused significant damage to bridges,
57 hydropower stations, and roads. Previous studies have primarily focused on the characteristics of glacial lake
58 changes, the resulting outburst floods, risk assessments, and the causes of specific GLOF events [3-5]. As
59 glaciers continue to thin and retreat, the glacial lakes they feed are expanding rapidly [6-8]. Some studies
60 suggest that this expansion may increase the risk of GLOF triggers [9, 10]. While some research on past events
61 indicates that glacial lake growth and GLOF triggers are only weakly coupled [11-13]. The increasing
62 availability of optical satellite imagery, particularly with the launch of Landsat-8 and the Sentinel series since
63 2013, has provided an opportunity to refine our understanding of GLOF trends [12]. However, despite these
64 technological advancements, the development and implementation of effective mitigation strategies remain
65 limited in practice.

66 GLOF risk is determined by event frequency and magnitude, as well as downstream exposure and
67 vulnerability [9, 14]. With increasing socio-economic activities and expanding infrastructure in high mountain
68 regions, future GLOF exposure is expected to rise, posing a significant challenge for sustainable mountain
69 development [15]. Although engineering interventions such as Tsho Rolpa's siphon system, and community
70 preparedness efforts, like Chungthang's training program [16, 17], GLOFs continue to cause severe
71 downstream damage ([Table S1 online](#)). This persistent threat can be attributed to three systemic challenges:
72 (1) inadequate monitoring and early warning systems (EWS) for widely distributed high-risk lakes [18], (2)
73 limited engineering coverage due to financial and logistical constraints in harsh regions ([Table S2 online](#)), and
74 (3) delayed emergency response, which hinders the timely dissemination of warnings to affected communities,
75 including those in transboundary areas [19]. Therefore, a reliable and adaptable approach is urgently needed
76 to address these challenges across the Himalaya region.

77 Since 2019, China has implemented a Glacial Lake Management System (GLMS) to enhance GLOF disaster
78 prevention and mitigation. This system integrates EWS, engineering interventions, and a structured framework
79 for capacity building and responsibility ([Fig. 1](#)). A key feature of the GLMS is the assignment of specific
80 personnel for lake management and protection, ensuring coordination across governmental and local levels.
81 This systematic approach facilitates rapid information exchange among stakeholders, including local
82 communities and decision-makers, which improves the effectiveness of disaster response. With several years
83 of successful operation, the GLMS presents a compelling model for exploring how integrated management
84 strategies can address the region's escalating cryospheric challenges.

85 This study is timely in assessing the effectiveness of China's GLMS and its potential for broader
86 application across the Himalaya. By integrating historical GLOF trends (1990–2023), future projections, and
87 practical mitigation strategies, we assess the GLMS's effectiveness and propose an integrated technical-
88 sociopolitical framework for regional GLOF risk reduction. Combining strategic engineering, community-
89 driven EWS, and transboundary governance, this framework provides scientific insights and actionable

90 guidance for sustainable mountain development and cooperation amid escalating glacier-related geohazards
91 in high-altitude regions.

92

93 **2. Data and Methods**

94 **2.1 GLMS framework**

95 China's GLMS, is a specialized component of China's national River and Lake Chief System, which has
96 been implemented nationwide since 2019 [20]. GLMS is a structured and top-down framework designed to
97 mitigate GLOF risks, through integrated monitoring, engineering interventions, and governance. The system's
98 architecture comprises four key components: inputs, intermediate parameters, functions, and outputs,
99 coordinated across governmental, local, and community levels (Fig. 1).

100 Inputs: The GLMS relies on near real-time data from optical/SAR satellite imagery (e.g., Landsat-8,
101 Sentinel series, Planet, Gaofen series), UAV-based observations, on-site lake monitoring stations, and
102 community reports. These data sources provide information on lake area, volume, dam stability, and potential
103 triggers (e.g., landslides, avalanches).

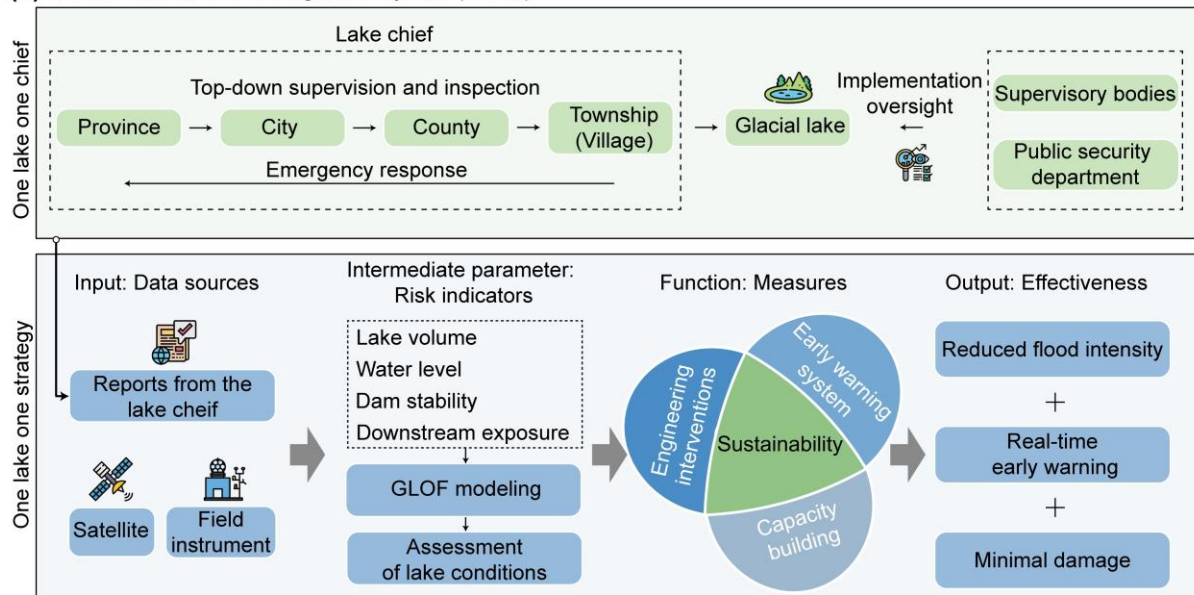
104 Intermediate parameters: Risk assessments integrate input data to prioritize high-risk lakes based on
105 factors such as lake volume, dam integrity, and downstream exposure. These parameters guide decision-
106 making for intervention strategies.

107 Functions: The GLMS operates through three core functions: (1) EWS: Automated alerts based on
108 monitoring data, disseminated to local authorities and communities via mobile networks and alarms. (2)
109 Engineering interventions: Active measures, such as siphon drainage or spillway construction, and passive
110 defenses, like embankment reinforcement, to reduce lake volumes and flood intensity. (3) Governance and
111 capacity building: Dedicated personnel are assigned to lake management, ensuring coordination between
112 central government, local agencies, and communities. Training programs and emergency drills enhance
113 preparedness.

114 Outputs: The GLMS aims to reduce GLOF impacts, including minimal damage to infrastructure (e.g.,
115 buildings, roads, and bridges), reduced fatalities, and timely evacuations.

116 The system's architecture facilitates rapid information exchange and decision-making, enabling proactive
117 risk mitigation. For example, monitoring data feeds into risk assessments, which trigger EWS alerts or
118 engineering interventions, with governance ensuring stakeholder coordination. To assess the GLMS's
119 effectiveness, we employed two complementary approaches: (1) a comparative analysis of GLOF damage
120 trends within and outside China before and after GLMS implementation in 2019, and (2) controlled modeling
121 experiments for definitive effectiveness assessment, simulating disaster reduction with and without GLMS
122 engineering measures.

(a) China's Glacial Lake Management System (GLMS)



(b) Examples of mitigation measures in China



124

125 **Fig. 1.** Architecture of China's GLMS. (a) Coordination of data inputs, risk assessments, functions (monitoring, 126 engineering, governance), and outputs (reduced GLOF impacts) at the governmental and local levels through 127 top-down implementation frameworks. It operates at multiple administrative levels (province, city, county, 128 township, village) ensuring coordinated management. "One Lake, One Chief" and "One Lake, One Strategy" 129 are principles from China's water management system ensuring each glacial lake has dedicated official 130 responsibility for monitoring and safety management, customized risk management plans based on specific 131 lake characteristics (volume, dam stability, downstream exposure) and tailored interventions rather than 132 uniform approaches across all lakes. This creates personalized, accountable glacial lake safety systems with 133 site-specific solutions. (b) Examples of mitigation measures in China. All the lake locations in (b) are marked 134 in Fig. 2.

135

2.2 Updated historical GLOF inventory and frequency

137 To assess the trends and impacts of GLOFs across the Himalaya, including the Hindu Kush, Karakoram,
138 Himalaya, Nyainqêntanglha, and Hengduan mountains, we updated the inventory of historical GLOF events.
139 We compiled existing GLOF datasets from peer-reviewed literature, government and institutional reports,
140 news sources, expert interviews, and geomorphic evidence to ensure dataset comprehensiveness and
141 reliability [21–23]. To ensure the accuracy of event identification, we analyzed long-term remote sensing data
142 and cross-validated changes in lake extent with multiple imagery sources (Landsat MSS/TM/OLI and Sentinel-
143 2 imagery with less than 20% cloud cover) for each identified glacial lake. Because sudden reductions in lake
144 surface area can also result from non-GLOF factors such as seasonal drawdown or transient cloud and shadow
145 cover. In addition, a qualitative assessment of the geomorphic conditions before the event was conducted
146 through NASADEM, including the steepness of the slopes around the lake and the integrity of the dam, to
147 diagnose potential GLOF triggers and verify the characteristics after the event. Historical GLOF events from
148 1990 to 2023 were detected by identifying sudden reductions in lake area and associated geomorphological
149 changes, such as breach formation, deposition of debris fans, and channel erosion [24] ([Figs. S1 and S2 online](#)).
150 If the pre- and post-event images were from different years, we assigned the event to the year of the post-
151 event image. To evaluate the impacts of GLOFs, we systematically recorded damage to downstream
152 populations and infrastructure, including roads, bridges, and buildings. Special attention was given to
153 analyzing spatial and temporal variations in GLOF-related damage inside and outside China, particularly after
154 the full implementation of the GLMS in China since 2019.

155 Assessing long-term trends in GLOF activity is challenging due to inconsistencies in historical records.
156 Variations in criteria and methodologies used to identify and catalog GLOFs have led to discrepancies among
157 studies [21, 23, 25]. Additionally, improved satellite data coverage and increased research attention have led
158 to the identification of smaller GLOFs that were previously overlooked [26], potentially biasing frequency
159 analyses [24]. Using the updated GLOF dataset, we reassessed the temporal trends of historical Himalaya
160 GLOFs. Due to the incompleteness of early records, our analysis focused on events occurring after 1990, when
161 research activity became more consistent and comprehensive [26] ([Fig. S3a online](#)). To mitigate potential
162 biases introduced by variations in satellite image availability, we employed two independent methods to
163 assess changes in GLOF frequency over time [12].

164 *Method I: Normalization based on image availability:* This approach evaluated the regularity of annual
165 GLOF events in lakes with sufficient satellite imagery. We defined "adequate imagery" using the interquartile
166 range (IQR) of time intervals between pre- and post-GLOF images. The standard based on IQR can effectively
167 eliminate the influence of outliers and utilize the statistical properties of IQR to reasonably categories image
168 data availability, ensuring the robustness and reliability of the analysis results [12]. Specifically, we set
169 thresholds of 48 and 240 days for the 25th and 50th percentiles, respectively ([Fig. S3b online](#)). Lakes with at
170 least one pair of images separated by 48 days (or 240 days) were classified as having sufficient imagery. To
171 account for differences in image availability, we normalized GLOF frequency by computing the ratio of
172 detected GLOF events to the number of lakes with sufficient imagery per year, for each threshold.

173 *Method II: Standardization at constant image availability:* To further control for biases related to image
174 frequency, we used a bootstrap resampling method to assess trends under a fixed number of available images
175 per year. We randomly selected a constant number of images per year (50 and 100 images), recorded the

176 number of GLOF events detected, and fitted a linear trend to estimate changes in event frequency over time
177 (Fig. S3c online). This process was repeated 10,000 times to capture variability in trend estimates.

179 **2.3 GLOF simulations**

180 Our GLOF simulations focused on flood changes before and after engineering measures implementation.
181 We conducted simulations using two complementary models: r.avaflow and HEC-RAS. r.avaflow, an open-
182 source GIS framework, was selected for the Jialong Co case study due to its ability to dynamically simulate
183 complex process chains, including ice avalanches, lake outbursts, and debris flows, with high fidelity in site-
184 specific scenarios (Text S1 online). HEC-RAS was used for region-wide simulations of 43 high-risk proglacial
185 lakes, as future landslide zones, shifting with glacier retreat, are uncertain, and its hydrological modeling
186 ensures comparability across diverse Himalaya terrains (Text S2 online). This dual approach enabled to assess
187 both the detailed effectiveness of GLMS interventions at a single lake and the broader regional implications
188 of mitigation strategies. Jialong Co, a glacial lake in the Poiqu River basin, poses a significant high-risk level if
189 impacted by an ice avalanche. A potential outburst flood could severely affect Nyalam town and downstream
190 areas in Nepal [27]. Following the implementation of the GLMS, local authorities took proactive measures to
191 lower the lake's water level to mitigate this risk (Fig. S4 online). To model the potential evolution and impacts
192 of a GLOF at Jialong Co, we used the open-source GIS simulation framework r.avaflow [28], which dynamically
193 simulates landslide-lake interactions and debris flow hydraulics. The model has previously been applied to
194 simulate complex process chains, such as the 2012 Santa Cruz GLOF involving multiple lakes [29] and the 1962
195 and 1970 Huascarán landslides [30], demonstrating its capability in simulating process transformations at
196 system boundaries. In this study, we performed simulations for both pre- and post-mitigation conditions,
197 assuming an ice avalanche impact scenario originating from the steep adjacent glacier.

198 The model setup incorporated several key inputs. The avalanche source was identified as the glacier
199 tongue, which is highly susceptible to collapse due to its crevassed and steep surface. The global glacier ice
200 thickness dataset, which is based on a consensus of five different ice thickness models, was used to calculate
201 the volume of the potentially unstable area [31]. The estimated avalanche volume was approximately 1.9×10^7
202 m^3 . Terrain data were derived from the global TanDEM-X Digital Elevation Model (DEM), which shows superior
203 performance compared to NASADEM in Jialong Co case study using r.avaflow, was specifically employed for
204 modeling potential GLOF scenarios. Lake bathymetry and volume were obtained from a 2019 uncrewed
205 surface vessel (USV) survey, referencing the WGS 84 UTM zone 45N coordinate system. The estimated lake
206 volumes before and after water level reduction were calculated using Landsat OLI boundary vector data,
207 assuming a constant lake bed, and processed with the surface volume tool in ArcGIS 10.2 [32]. Material
208 properties were defined for the different components of the flow. The initial avalanche was modeled as a two-
209 phase flow, consisting of a solid phase (ice: $\rho=900 \text{ kg m}^{-3}$) and a liquid phase (lake water: $\rho=1000 \text{ kg m}^{-3}$). The
210 moraine dam was designated as an entrainment zone composed of a solid phase (moraine: $\rho=2700 \text{ kg m}^{-3}$)
211 [27]. Entrainment was simulated using a simplified model, where the entrainment rate is proportional to flow
212 momentum and an empirical entrainment coefficient was set $10^{-6.5}$ [28]. However, for the post-mitigation
213 scenario, we assumed that entrainment did not occur, as the dam had been strengthened and sediment
214 deposition into the lake was not considered [27]. Friction parameters were defined based on the nature of the

215 flow. During the initial avalanche stage, the basal friction angle was set to $\varphi = 25^\circ$, with an internal friction
216 angle of $\delta = 10^\circ$. For the flow process beyond the moraine, where the flood transforms into a water-saturated
217 debris flow, we adjusted the internal friction angle to $\delta = 1^\circ$, while keeping the basal friction angle at $\varphi = 25^\circ$
218 [33]. The total simulation time was set to 1200 seconds, allowing sufficient time for the flood to travel
219 downstream. To assess the potential impacts on downstream areas, we extracted flow characteristics such as
220 flow depth and velocity by defining a cross-section along the flow channel at Nyalam town. This provided
221 insights into the flood behavior and its potential consequences for local infrastructure and communities.

222 Future GLOF simulations were conducted exclusively for very high-risk glacial lakes [15]. Only proglacial
223 lakes were modeled due to their susceptibility to external influences, and lakes with a projected future area
224 smaller than 0.1 km^2 were omitted to minimize uncertainties. Given the impracticality of investigating all
225 possible lake failure triggers in the field, we assumed a generalized scenario. To model GLOFs, the potential
226 drainage volume of each lake (V_d) was determined based on its total volume (V_0) using the empirical
227 relationship [9]:

$$228 \quad V_d = 1.14V_0^{0.74} \quad (1)$$

229 Peak discharge (Q) was estimated using a well-established nonlinear relationship derived from statistical
230 data [34]:

$$231 \quad Q = 0.045V_d^{0.66} \quad (2)$$

232 Based on the estimated drainage volume and peak discharge, a hydrological break curve was obtained,
233 assuming that drainage volume changes linearly over time [35]. Previous studies have shown that this
234 assumption does not significantly impact flood evolution [36–38]. The length of the flood impact track (L) was
235 derived from the drainage volume using the empirical equation [11]:

$$236 \quad L = 12.61V_d^{0.38} \quad (3)$$

237 We employed freely available NASADEM (30 m) to perform extensive GLOF simulations in the complex
238 terrain of the Himalaya due to the better consistency compared to global TanDEM-X DEM, which exhibits
239 anomalous values in many regions [39]. Model parameter selection was guided by a preliminary sensitivity
240 analysis, setting the minimum computational unit to 30 m, the Manning coefficient to 0.05, and ensuring a
241 simulation runtime exceeding 10 hours to allow sufficient flood propagation. The HEC-RAS model was used
242 to compute the inundation area, maximum depth, and velocity, as it has been validated in numerous studies.

243 To quantify GLOF intensity, we defined an indicator (H) following Maranzoni et al. [40]:

$$244 \quad H = hv \quad (4)$$

245 where h is the maximum flood depth at a given location and v is the maximum velocity. Floods were classified
246 into four intensity levels—low, medium, high, and extreme—based on velocity and depth. Given the elevated
247 flood risks in the Himalaya region with its steep valleys and high relief, an intensity threshold of 10 was set for
248 the "extreme" flood class.

250 **2.4 Predicting the future development of glacial lakes and validation**

251 Proglacial lakes form adjacent to glacier termini, primarily as moraine-dammed lakes, blocked by
252 sediment and debris in deglaciated areas, or ice-dammed lakes, blocked by ice in actively glaciated regions.
253 In the Himalaya, moraine-dammed proglacial lakes predominate, posing the highest GLOF risk and persisting

in retreating glacial landscapes [23, 32]. Given the projected increase in these lakes due to climate-driven glacier retreat, our study focuses on moraine-dammed proglacial lakes to predict their future development and inform hazard mitigation [15, 41]. Our proglacial lake prediction model consists of two main components: an ice thickness module and a subglacial depression module. The model is implemented in MATLAB, with the ice thickness module developed in this study and the depression module adapted from a previous study [42]. The model iterates between estimating subglacial depressions and constraining the ice thickness until the parameters converge ([Figs. S5 and S6 online](#)).

Accurate estimation of subglacial depressions relies on the precise modeling of present ice thickness and bedrock topography [43]. In this study, we re-implemented the mass conservation model by Huss and Farinotti [44] to estimate ice thickness for all lake-terminating glaciers, as this approach has demonstrated robustness against errors in input datasets such as DEMs and glacier boundaries [45] ([Text S3 online](#)). The model inputs include NASADEM and modified Randolph Glacier Inventory (RGI) 6.0 data. We utilized NASADEM due to its high temporal consistency, representing glacier topography in 2000. By coupling this with corresponding glacier boundaries from the same period, we can accurately derive glacier thickness and identify subglacial depressions (potential future lake formation sites) while avoiding thickness modeling errors that could arise from temporal inconsistencies between glacier boundaries and topographic data [44]. While most parameters remain consistent with the original model [44], we modified the approach for determining the sliding F_{sl} and correction parameters to better account for variations in glacier dynamics.

One key modification involves incorporating the influence of meltwater lubrication at the terminus of lake-terminating glaciers, which enhances basal sliding. In the original model, the sliding factor is empirically derived based on glacier size and remains constant across the entire glacier. Here, we introduced a more localized approach by defining the sliding parameter for each 10-m elevation band within the model. Specifically, we assumed that the basal sliding ratio of glacier ice in direct contact with a glacial lake should not exceed 0.9, and we applied an inverse tangent activation function to gradually reduce the sliding ratio to 0.2 near the equilibrium line (Equation 1). This ensures a higher sliding ratio near the lake, with a rapid decrease as the distance from the lake increases. The accumulation area ratio was set to 0.44 for the entire Himalaya, following the findings of Miles et al. [46].

Despite these refinements, the sliding ratio remains an empirical parameter, and the actual conditions may vary across different glaciers. To improve model reliability, we introduced three additional constraints to refine and correct predictions. These constraints help ensure that the estimated ice thickness and subglacial depressions align with observed glacier behavior and known physical processes.

$$fsl(h_{(normalizing)}) = 1 - (e^{h_n} + e^{-h_n}) / (e^{h_n} + e^{-h_n}) \quad (5)$$

where h_n is a normalizing elevation.

Thickness measurements of glacial contact lakes are difficult and limited by terminus topography ([Fig. S7 online](#)). To refine the accuracy of our model, we applied three key constraints to correct and validate the simulated ice thickness and future lake development. First, we accounted for the discrepancy between the observed elevation change at the glacier terminus and the actual ice thickness. The elevation changes of lake-terminating glacier termini, as derived from remote sensing, only represents the thickness of ice above the water surface (H_{ow}), which is less than the full ice thickness (H_g). To ensure realistic estimates, we required that

293 the simulated glacier thickness in the expanding portion of the glacial lake (2000–2020) exceeded the
294 observed elevation change (d_H) obtained from remote sensing datasets [47]. We validated this elevation
295 change estimates using TanDEM-X CoSSC and NASADEM datasets at Galong Co, achieving a high correlation
296 ($R^2=0.85$, RMSE=7.8 m) ([Fig. S8 online](#)). Since ice thickness models often underestimate thickness near glacier
297 margins due to interpolation effects [48], we introduced a 90% threshold correction, which yielded optimal
298 estimates when compared to in-situ ice thickness measurements.

299 Second, we constrained the modeled subglacial depression by ensuring that its extent in contact with
300 the proglacial lake was larger than the observed glacial lake expansion from 2000 to 2020. This prevented
301 underestimation of future lake growth by requiring the model to account for real-world trends in lake
302 expansion. Third, we refined the final iteration of the model by minimizing the error between the simulated
303 glacial lake volume growth (2000–2020) and the volume calculated using the area-volume scaling method
304 [32]. This ensured that the modeled lake evolution was consistent with empirical data. By integrating these
305 constraints, we derived the distribution and depth of subglacial depressions connected to proglacial lakes.
306 Combining this information with the observed glacial lake extent in 2020, we determined the projected future
307 extent of each glacial lake under continued deglaciation.

308 Nine glaciers were selected for model validation as they possess independent geodetic measurements
309 and corresponding lake bathymetry datasets, enabling the calculation of glacier thickness at the terminus.
310 The geodetic method determines glacier thickness changes above the water surface (H_{ow}) by subtracting two
311 or more DEMs. The ice thickness below the water surface corresponds to the depth of the glacial lake (H_{sub})
312 formed after the glacier retreats. Bathymetric data were collected using an USV during fieldwork from 2017
313 to 2021. By summing H_{ow} and H_{sub} , we reconstructed glacier thickness for the year 2000 (H_g), assuming minimal
314 sediment infill over this period. Two of the examined glacial lakes, Ranzeria Co and Jiweng Co, experienced
315 outburst events in 2013 and 2021, causing water level drops of ~20.2 m and ~25.8 m, respectively [49]. Since
316 bathymetry data were measured post-outburst, these drops were added to the measured depths to estimate
317 pre-outburst lake depths.

318 Although our model predicts the maximum possible extent of future glacial lakes, factors such as ice
319 thickness uncertainties, sediment accumulation, and outlet variations may prevent lakes from reaching these
320 extents. Increasing glacier thickness deepens subglacial depressions, sometimes merging isolated depressions
321 and expanding projected lake areas. Remote sensing data from 2000 to 2020 were used to validate the
322 modeled extents of subglacial depressions. Underestimated ice thickness resulted in smaller depressions,
323 making this validation approach viable, whereas overestimated ice thickness posed challenges. To assess the
324 sensitivity of ice thickness on lake projections, we scaled glacier thickness in 10% increments from 50% to
325 150% ([Fig. S9 online](#)). Using these thickness variations, we computed corresponding changes in lake extent
326 and volume and estimated the sensitivity.

327

328 **3. Results**

329 **3.1. Initial performance of GLMS implementation**

330 To evaluate the effectiveness of the GLMS, we compare downstream damage caused by GLOFs within
331 China to those outside China across the Himalaya. Both regions have comparable numbers of proglacial lakes,

historical GLOFs, and future high-risk lakes [15, 32], which facilitates a meaningful comparative analysis. We updated and validated previous regional GLOF inventories [9, 21-23], excluding 62 cases with no confirmed and clear evidence of an outburst ([Fig. S10 online](#), [Table S3 online](#)). Considering all types of dams, including moraine, ice, and other natural barriers, we compiled a comprehensive GLOF dataset spanning 1990 to 2023, consisting of 59 events within China and 93 events outside China ([Fig. 2a](#), [Table S1 online](#)). Most events were concentrated in the Central Himalaya and Karakoram, with 92% of GLOF events in the Central Himalaya originating from moraine-dammed lakes.

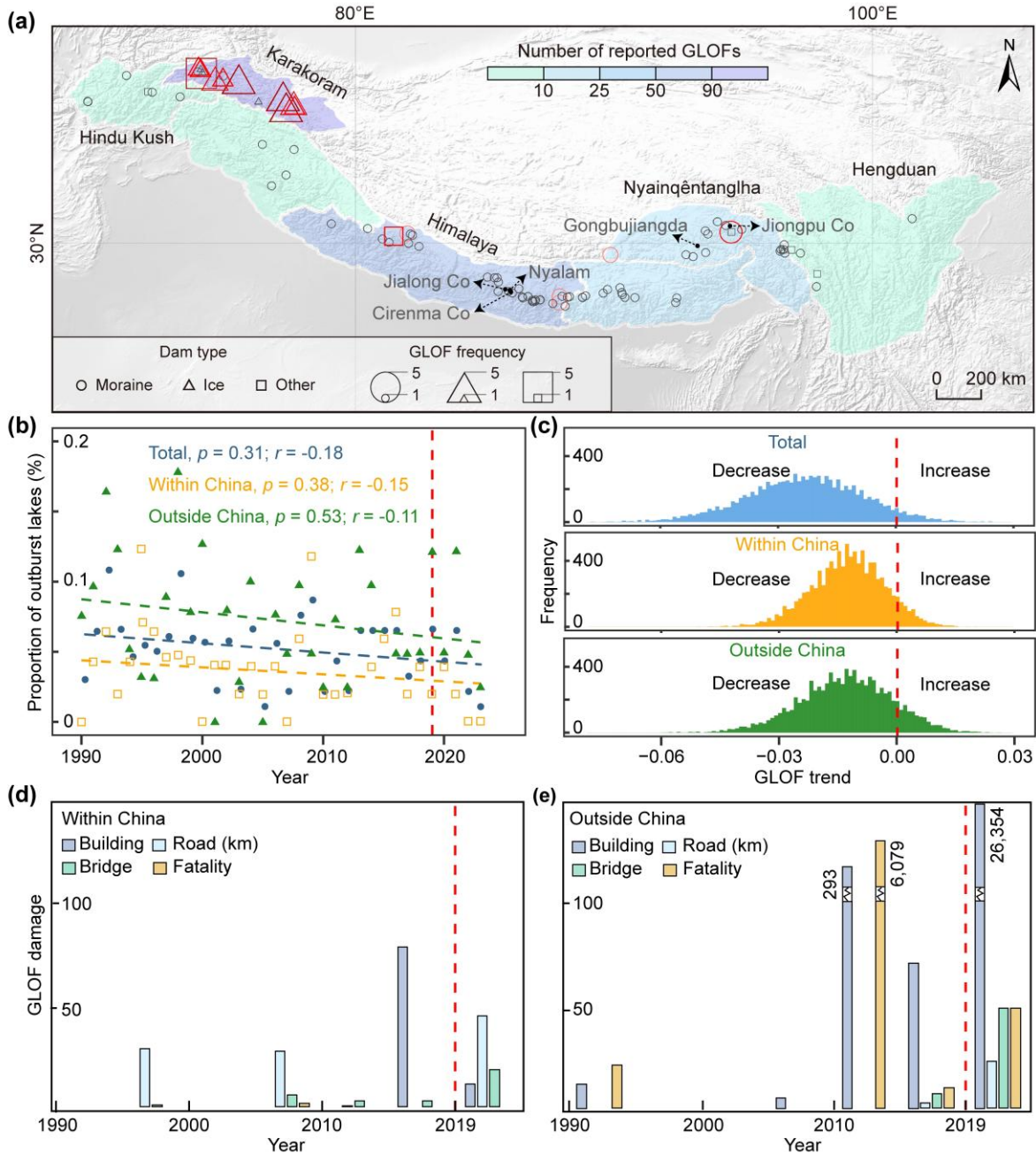
To assess temporal trends in GLOF activity, we employed two independent methods to account for biases introduced by variations in image availability ([Fig. 2b-c](#)). First, we analyzed the annual number of GLOFs and the proportion of lakes that experienced GLOFs each year. Both indicators showed statistically insignificant decrease trends over time, respectively, with the best-fit linear trends close to zero. Second, we applied a bootstrap method to further correct for potential biases related to image availability [12], which similarly showed no increasing trend in GLOF frequency over time. Separate analyses for regions within China and outside China yielded consistent findings, with no significant temporal changes in event occurrence ([Fig. 2b-c](#)), despite the ongoing acceleration of glacier thinning and retreat, and the continued expansion of both the number and area of glacial lakes ([Fig. S11 online](#)).

Although the frequency of GLOFs has remained stable, the resulting damage to downstream communities, such as buildings, bridges, roads, and human lives, has intensified, primarily due to rising exposure and vulnerability ([Fig. 2d-e](#)). Prior to 2005, only minor damage was reported in association with 10 GLOFs. However, as downstream populations have grown and infrastructure has expanded, exposure to these events has increased, leading to a corresponding rise in their impacts. After 2005, 31 GLOFs recorded in China, six GLOFs in China caused significant damage, including the destruction of at least 88 buildings, damage to 71.4 km of roads, destruction of 30 bridges, and two fatalities. This trend is even more pronounced in regions outside China. Of the 51 GLOFs recorded, 15 caused damage to at least 26,721 buildings, nine affected 32.5 km of roads, 14 damaged 65 bridges, and five events resulted in 6149 fatalities.

From the implementation of GLMS in 2019 to 2023, four GLOFs have occurred in China (Kyagar lake, Jiweng Co, and two unnamed lakes), with only one causing downstream damage—the 2020 Jiweng Co event. Notably, the village head received advance warning from an upstream villager about the glacial lake burst, enabling downstream villagers to evacuate to higher ground. Despite heavy infrastructure damage, no lives were lost, demonstrating the effectiveness of the EWS incorporating community patrols. Community participation and timely early warning mechanisms, where local managers successfully issued warnings for glacial lake outburst events, demonstrating the advantages of the "One lake, One chief" responsibility system in GLMS. In contrast, of 16 GLOF events occurring outside China after 2019, seven caused damage to over 60 people, 58 bridges, 30 kilometers of roads, and 26,354 buildings, indicating the potential protective benefits of systematic GLOF management systems. Available data suggests positive indications for China's GLMS performance, with reasonable grounds to expect similar systems could improve GLOF risk conditions elsewhere. However, definitive evidence remains limited due to the short observation period since 2019, infrequent GLOF occurrence leading to weak statistical power, and numerous confounding factors including different geological conditions, exposure patterns, and reporting systems across regions [50]. To address these

371 limitations in regional comparisons and provide more conclusive evidence, we conduct controlled modeling
 372 experiments at specific glacial lakes in the following analysis, which eliminate confounding factors by
 373 maintaining identical environmental conditions while varying only the management interventions.

374



375

376 **Fig. 2.** Historical GLOF trends and damage in the Himalaya. (a) Spatial distribution of historically reported
 377 GLOFs within China and outside China across the Himalaya, categorized by dam type. The number of recorded
 378 GLOFs in each subregion of the Himalaya is distinguished by varying background fill colors. (b–c) Trends in all
 379 recorded GLOFs compared to those occurring within China and outside China. The left panels show the
 380 proportion of lakes that burst in a given year, calculated as the ratio of reported GLOF events to the number
 381 of lakes with sufficient satellite imagery. The right panels display the distribution of trends over time based
 382 on bootstrapping, where 50 satellite images per year were randomly sampled, and event trends were

383 computed 10,000 times. In all cases, the trend slope remains below zero (x-axis), indicating no increasing trend
384 in GLOF occurrence over time when accounting for satellite image availability. (d–e) Damage to buildings,
385 roads, bridges, and populations caused by GLOFs since 1990 within China and outside China, aggregated over
386 5-year periods.

387

388 **3.2. Projected intensification of GLOFs in absence of GLMS**

389 Understanding the future intensity of GLOFs is critical for assessing downstream risks and informing
390 mitigation strategies. To achieve this, we developed a vertically and horizontally constrained ice-thickness
391 inversion model that integrates lake expansion and terminal elevation changes (see [Methods, Fig. S12 online](#)).
392 The simulated ice thicknesses for the nine glaciers demonstrated strong agreement with observed values, with
393 correlations ranging from 0.55 to 0.94 and root-mean-square errors (RMSE) between 5.0 and 36.1 m ([Fig. S13
394 online](#)). Our projections indicate that the maximum area of existing proglacial lakes will reach approximately
395 ~377.7 km² once glaciers and glacial lakes detach, nearly three times the extent mapped in 2000 (~123.2 km²)
396 ([Fig. 3](#)). The projected increase in lake area and volume is about 251.3 km² (+200%) and 11.8 km³, respectively,
397 compared to their 2000 levels. Potential growth after 2020 is estimated to be approximately 178.4 km² and
398 8.7 km³, representing 244% and 284%, respectively, of the changes observed from 2000 to 2020 ([Fig. 3](#)).

399 Future glacial lake expansion is expected to vary significantly in both spatial patterns and sizes. The
400 Central Himalaya, Nyainqêntanglha, and Eastern Himalaya will experience the largest increases in lake area,
401 accounting for 38.6%, 24.0%, and 17.6% of the total expansion, respectively. These patterns closely mirror the
402 projected trends in water volume. Most lakes in the 0–0.1 km² range (77%, n=641) have limited potential for
403 further expansion ([Fig. S14 online](#)). The most significant contributions to lake growth will come from those in
404 the 0.5–2.5 km² size range, with approximately half of these lakes projected to grow. In contrast, larger lakes
405 show limited potential for future expansion. Of the 10 lakes larger than 2.5 km², five are already constrained
406 by topographic limitations, leaving less than 10% capacity for further growth. Overall, the potential for future
407 glacial lake expansion in the region will be driven by a minority of lakes. Notably, just 25% of lakes will account
408 for 84% of the total area growth and 88% of the total volume increase, highlighting the need for targeted
409 mitigation measures.

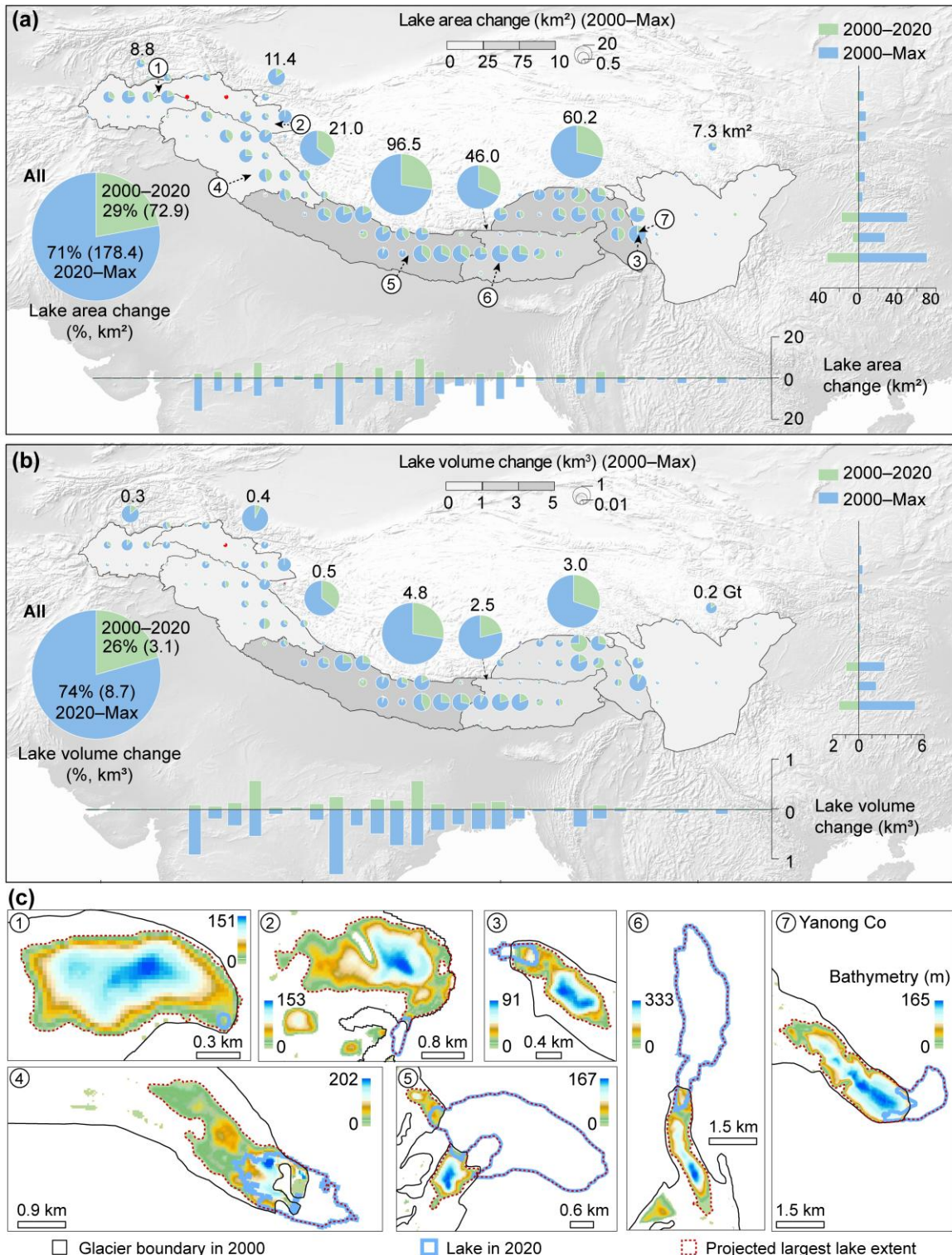
410 Given the projected expansion of glacial lakes and their potential to amplify downstream flood risks,
411 assessing the future intensity of GLOFs from high-risk lakes is crucial for prioritizing mitigation efforts. We
412 modeled future GLOFs for 43 high-risk proglacial lakes ([Table S4 online](#)), over half of which (56%) are in the
413 Central Himalaya and 21% in the Eastern Himalaya ([Fig. 4](#)). Without additional engineering interventions, their
414 area and water volume are expected to increase by 48% and 43%, respectively. Of these changes, 57% of area
415 growth and 50% of volume growth will occur in China, compared to 37% and 34% outside China.
416 Consequently, future flood intensity, defined as flow depth multiplied by velocity, is projected to rise by over
417 27%, with increases of 26% in the Central Himalaya and 22% in the Eastern Himalaya. Specifically, GLOF
418 intensity is expected to increase by 21% for 25 lakes within China and by 40% for 18 lakes outside China ([Table
419 S5 online](#)). These findings suggest that regions outside China may experience greater increases in GLOF
420 intensity.

421

422 **3.3. Mitigating future GLOF risk through GLMS implementation**

423 Mitigating future threats is critical to safeguard downstream regions, given the projected rise in GLOF
424 intensity from high-risk lakes. Engineering measures, specifically targeted at GLOFs through China's GLMS,
425 can substantially reduce disaster risks. We simulated the GLOF process for Jialong Co before and after a 20-
426 m water-level reduction ([Fig. S4 online](#)). The modeled peak discharge decreased by 50%, from 2×10^4 to 1×10^4
427 m^3/s , significantly reducing the flood impact on the town of Nyalam. If the same engineering measures applied
428 across all high-risk glacial lakes in the Himalaya could reduce their total area and volume by approximately
429 25% and 28%, respectively. The Central Himalaya has the highest potential for reduction, with projected
430 decreases of 30% in lake area and 32% in volume compared to lakes without engineering interventions. High-
431 risk lakes inside and outside China could expect reductions of 24% vs. 27% in area and 27% vs. 30% in volume,
432 respectively.

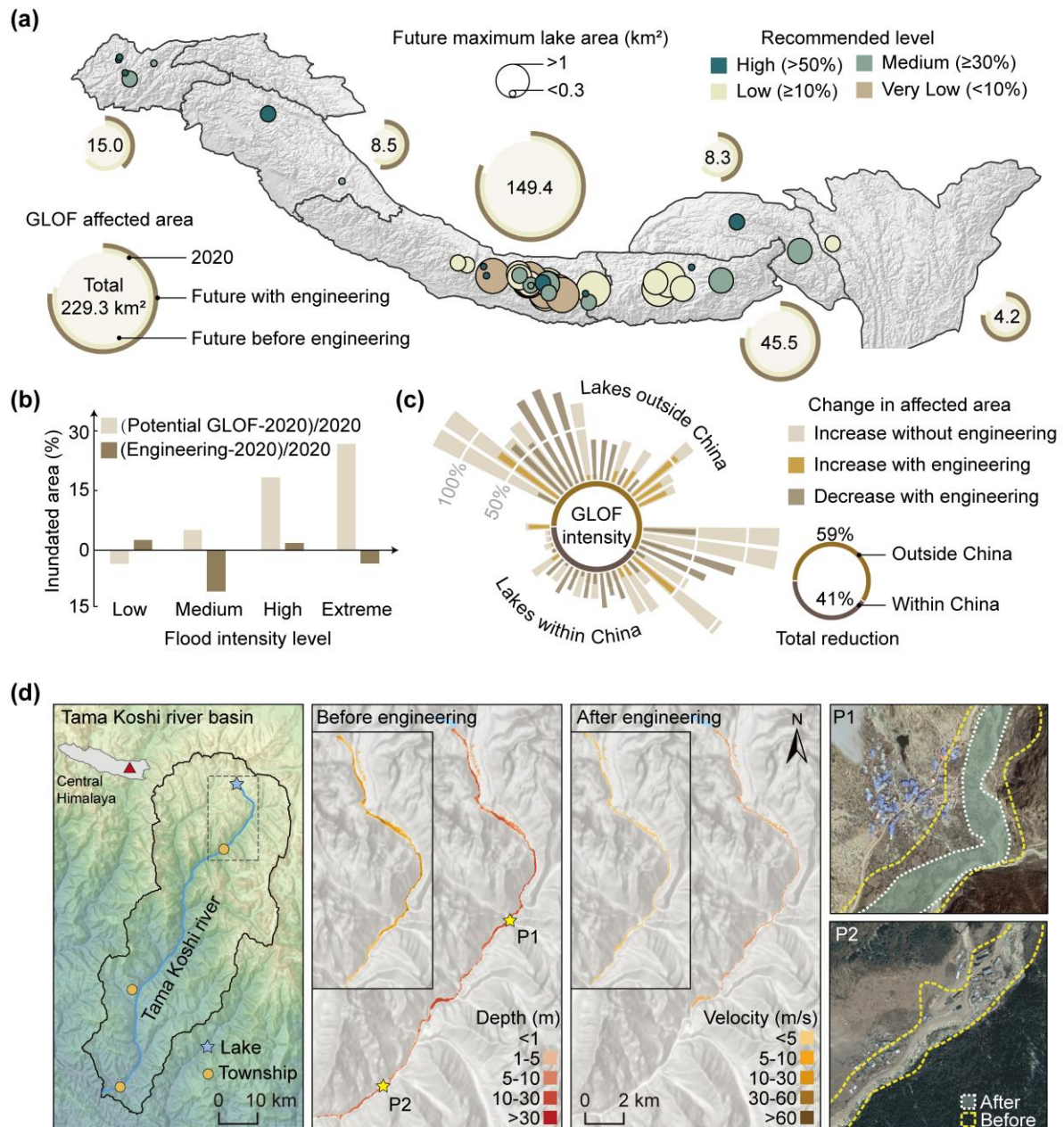
433 Engineering measures that reduce lake water volumes can significantly decrease potential flood runoff
434 distance, flow intensity, and inundation width along both riverbanks ([Fig. 4](#)). Future GLOF inundation areas
435 are projected to be reduced by 20% with engineering measures compared to without them. Implementing
436 the GLMS would significantly decrease GLOF intensity, particularly under extreme conditions, with the
437 magnitude of high and extreme intensity floods dropping by ~24%. Nearly a quarter of lakes would experience
438 a reduction in potential flood intensity exceeding 50% ([Table S6 online](#)). Regionally, the estimated reduction
439 is ~18% in the Central Himalaya and ~24% in the Eastern Himalaya. The GLOF intensity of high-risk lakes
440 could be reduced by ~21% inside China and ~29% outside China, highlighting the effectiveness of
441 engineering measures in GLMS in mitigating future GLOF hazards ([Fig. 4](#)).



443

444 **Fig. 3.** Future changes in existing glacial lake area and volume. (a) Projected future expansion of existing
445 proglacial lakes, using observed growth from 2000 to 2020 as a baseline. Lake growth trends along longitude
446 and latitude are also shown. (b) Same as a, but illustrating projected changes in glacial lake volume. Both lake
447 area and volume are expected to increase by over 300% compared to the 2000–2020 period, with the most
448 significant growth occurring in the Central Himalaya. (c) Predicted future lake extent and water depths of

449 maximum lake within each region. Locations are marked with triangular symbols with numbers in (a).
 450



451
 452 **Fig. 4.** Damage reduction before and after implementing GLMS engineering measures. (a) Reduction in flood
 453 intensity for potentially dangerous glacial lakes in each region, with proposed engineering interventions for
 454 each lake. Ten lakes are highly recommended for engineering, as flood intensity was reduced by over 50%
 455 with these interventions. (b) Changes in flood inundation area across different intensity levels. The extreme
 456 flood inundation area is projected to increase the most in the future but will also experience the greatest
 457 reduction after implementing artificial lake level management. (c) Changes in flood intensity from 2020 to the
 458 maximum projected extent, comparing scenarios with and without artificial measures. The total reduction in
 459 China represents the percentage change in the potentially affected area of lakes within China before and after
 460 engineering, relative to the change in the potentially affected area of all lakes. The impact of artificial measures
 461 on reducing the risk of potentially dangerous glacial lakes is more significant outside China than within China.

462 (d) Comparisons of the changes in flood depth, speed and intensity with and without artificial measures.
463 Artificial measures have a significant effect on reducing the risk of potentially risk glacial lakes. At location P2,
464 no floods reached this area after implementing the measures.

465 466 **4. Discussion**

467 **4.1 Uncertainties in GLMS performance**

468 Evaluating the effectiveness of China's GLMS in mitigating the GLOFs impact is subject to several
469 uncertainties due to the data limitations and model constraints. A primary source of uncertainty lies in
470 projecting glacial lake expansion, driven by variability in ice thickness estimates. Sensitivity analysis showed
471 that a $\pm 10\%$ variation in ice thickness altered projected lake area by $\pm 10\%$ but lake volume by $\pm 30\%$, with
472 extreme deviations (50% increase) yielding a 270% volume rise, while a 50% decrease reduced volume by 89%
473 ([Section 3.2, Fig. S9 online](#)). These discrepancies, stemming from subglacial topography and outlet elevation
474 in steep regions ([Fig. S15 online](#)), highlight the challenge of accurately modeling lake depth. Validation against
475 remotely sensed glacial lake extents from 2000 to 2020 shows that our thickness-based simulations align well
476 with observations, with errors between $7.5 \times 10^{-4} \text{ km}^2$ (25th percentile) and $1.1 \times 10^{-2} \text{ km}^2$ (75th percentile), and
477 a strong correlation ($R^2 = 0.99$) ([Fig. S16 online](#)). Comparisons with ice thickness estimates from Farinotti et al.
478 [51] and Millan et al. [52] revealed disparities, with predicted lake areas differing by -24% to +9% and volumes
479 by -59% to +102% ([Table S5 online](#)). Field observations also confirm our model's projections, showing
480 topographic constraints limit Jiongpu Co and Gangxi Co's expansion, unlike Laigu and Guangxie Co, while
481 inconsistent boundaries in Farinotti et al. [51] and Millan et al. [52] lead to inaccurate predictions ([Fig. S17](#)
482 [online](#)). Sediment accumulation, with $\sim 40\%$ of overdeepenings not forming lakes and 45% of new lakes
483 disappearing [53, 54], and GLOF-induced outlet elevation drops by $\sim 20 \text{ m}$ ([Fig. S18 online](#)) further obscure
484 volume projections, hindering accurate prioritization [49].

485 Last, the focus on engineering interventions excludes EWS and capacity building, which are hard to
486 quantify, and omits future exposure changes, suggesting the 20% flood intensity reduction is conservative
487 ([Section 3.3, Fig. 4](#)). Additional uncertainties stem from the comparative damage analysis (1990–2018 vs. 2019–
488 2023), where the relatively short post-2019 period limits the sample size, potentially reducing the statistical
489 power. However, we validated these findings through multiple approaches, including documented case
490 studies and complementary simulation analyses, which collectively support the robustness of our damage
491 reduction estimates. Simulation assumptions in r.avaflow and HEC-RAS ([Section 2.3](#)) oversimplify site-specific
492 dynamics, such as landslide-induced outbursts [55]. These limitations underscore the need for enhanced data
493 collection, longer-term monitoring, and adaptive strategies to optimize GLMS deployment.

494 495 **4.2 GLMS recommendations for high mountain regions across and beyond the Himalaya**

496 China's GLMS, implemented in 2019, has shown potential to mitigate GLOF impacts through integrated
497 monitoring, engineering, and governance ([Fig. S5 online](#)). However, high economic costs and inadequate
498 cross-border information sharing constrain GLMS scalability in the whole Himalaya region. We propose an
499 integrated technical-sociopolitical framework built on the GLMS's strengths while addressing its limitations to
500 provide a scalable solution for GLOF mitigation across the Himalaya ([Fig. 5](#)). The key differences include: (1)

501 emphasis on community-driven early warning systems vs. top-down approaches, (2) transboundary
502 collaboration mechanisms, and (3) distributed rather than centralized decision-making.

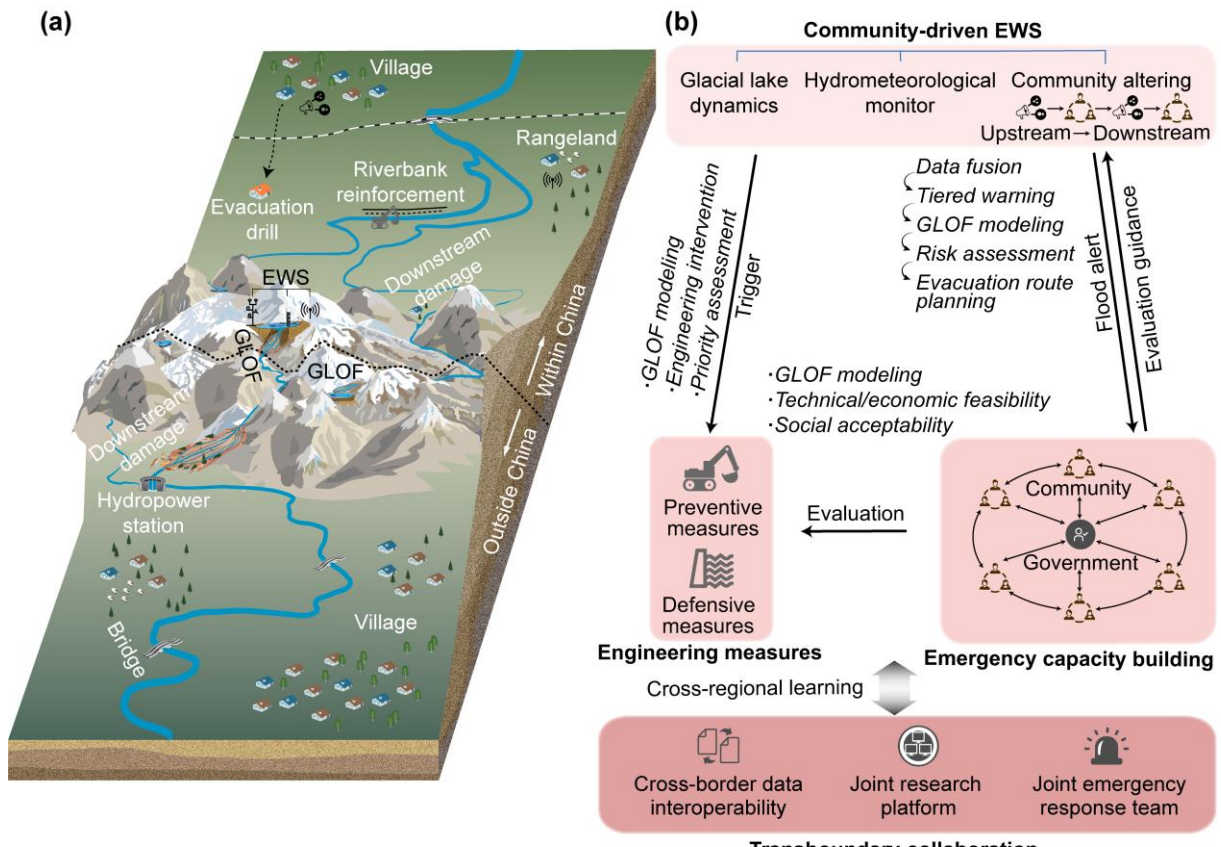
503 Large-scale engineering interventions for all high-risk lakes are neither feasible nor sustainable due to
504 high costs, logistical and technical constraints, and potential environmental consequences ([Fig. S19 online](#)).
505 While reinforced dams and spillways can reduce flood intensity, they do not eliminate risk entirely, as even
506 small outburst events can erode sediments and damage infrastructure [56, 57]. In some cases, engineering
507 measures may have minimal or even adverse effects [33, 58]. Given the high costs and site-specific challenges
508 of mitigation projects, a thorough feasibility assessment considering cost performance, the future lake
509 development and intervention effectiveness should be conducted before implementation. In this study, we
510 strongly recommend engineering interventions for lakes that have high development potential and pose
511 significant future GLOF threats ([Fig. 4](#)). Implementing these measures early will maximize benefits by
512 proactively reducing flood risks. The required water-level reductions to prevent downstream infrastructure
513 impacts can be estimated accordingly. In contrast, large-volume lakes with limited potential for further
514 expansion are not recommended for engineering interventions. Due to their substantial capacity and minimal
515 expected change, preemptive water release from these lakes would have little effect on overall risk, making
516 engineering the least effective mitigation option. Instead, EWS and other downstream measures should be
517 prioritized to manage potential hazards, such as Cirenma Co [18]. This reflects the experience of "one lake,
518 one strategy" principle in GLMS, where customized management approaches are tailored to each lake's
519 specific risk profile and cost-effectiveness considerations (Figure 1a).

520 Investments in EWS should prioritize reliability and targeted coverage for high-risk lakes, rather than
521 generalized deployment. Since the establishment of four EWS outside China, 15 GLOFs have occurred since
522 2019, seven of which caused significant infrastructure damage, and two resulted in fatalities ([Table S2 online](#)).
523 Despite the potential of EWS, their implementation still lags behind the number of high-risk glacial lakes [18].
524 Community-based, informal EWS can serve as an effective complement to formal systems, especially for
525 vulnerable communities. For example, during the Pemding Pokhari GLOF, upstream warnings of extreme
526 rainfall, flooding, and landslides enabled rapid evacuations, preventing casualties. Similarly, eyewitness alerts
527 allowed for a 30-minute evacuation during the 2020 Jiweng Co outburst in China, averting injuries. Despite
528 \$3 billion in Tibetan investments in flood control measures and drills, these efforts may have limited
529 effectiveness without reliable EWS support, as demonstrated by the 2023 South Lhonak Lake disaster in Sikkim
530 [5, 59]. These cases highlight the importance of integrating community-driven EWS with China's GLMS to
531 enhance reliability, coverage, and resilience, especially in areas where formal systems may fail ([Table S2 online](#)).

532 No single measure can fully mitigate GLOF risks in densely populated high-mountain regions. A
533 comprehensive strategy requires an integrated approach that combines various EWS, engineering
534 interventions, capacity-building initiatives, and active community engagement through awareness programs
535 and emergency drills ([Fig. 5](#)). China's GLMS offers a structured framework for regions that lack effective GLOF
536 mitigation strategies. Building such a comprehensive system is a complex task, involving the integration of
537 social, political, and environmental considerations, alongside strong governmental and societal support. While
538 the centralized governance model in China has been effective, it may not be easily replicable in neighboring
539 countries. Therefore, effective disaster management calls for regional cooperation between China and its

540 neighbors, emphasizing intergovernmental collaboration, joint research efforts, and enhanced data and
 541 information sharing [60].

542



543
 544 **Fig. 5. A new framework for GLOF mitigation across the Himalaya.** (a) A schematic diagram of the new
 545 framework. (b) A flowchart of the proposed new framework, which integrates community-driven EWS,
 546 engineering interventions, emergency capacity building and transboundary collaboration to effectively reduce
 547 future GLOF risk across the Himalaya. The framework emphasizes scientific hazard assessment and
 548 engineering feasibility evaluation as foundational elements for risk management decisions. Critical upstream-
 549 downstream information exchange, particularly across international borders, ensures timely warning
 550 dissemination and coordinated response efforts. The system incorporates real-time data fusion for risk
 551 assessment, tiered warning systems, and evacuation planning, with enhanced community emergency
 552 response capabilities through continuous training and capacity building programs. Key components include
 553 multi-level coordination from local community alerting and monitoring to regional cross-border cooperation,
 554 integrating both proactive mitigation measures and passive defense strategies through continuous feedback
 555 loops between government agencies and communities.

556

557 **5. Conclusions**

558 This study introduces China's GLMS and demonstrates its effectiveness in mitigating the GLOF damage
 559 across the Himalaya. Although the overall frequency of GLOFs has shown a weak decreasing trend over the
 560 past three decades, the damage to downstream communities and infrastructure has escalated due to rising

561 exposure and vulnerability. The GLMS exemplifies a proactive, integrated approach to GLOF mitigation. We
562 demonstrate that a combination of EWS, engineering interventions, and community preparedness measures
563 can significantly reduce GLOF risks. In particular, controlled water level drawdown has the potential to reduce
564 flood intensity by up to 24%.

565 Building on the proven effectiveness of GLMS and considering the transboundary nature of GLOFs, we
566 propose a holistic framework for region-wide risk management that integrates scientific research, engineering
567 solutions, policy frameworks, and community engagement. This framework emphasizes the urgent need for
568 enhanced regional disaster preparedness, improved land-use planning, and strengthened transboundary
569 cooperation.

570 The China's GLMS offers a valuable model for scaling up mitigation efforts in the Himalaya and beyond.
571 However, continued research and investment are critical to ensure the sustainability and regional applicability
572 of these solutions. By improving EWS, enhancing infrastructure resilience, and promoting international
573 cooperation, we can better protect vulnerable populations from glacier-related geohazards in a changing
574 climate.

576 **Competing interests**

577 The authors declare no competing interests.

579 **Acknowledgements**

580 This study was supported by grants from the National Natural Science Foundation of China (grant no.
581 42571153; 42301150; 42301140), the China Post-Doctoral Program for Innovative Talents (grant no.
582 BX20230387), the Basic Excellent Research Group for Tibetan Plateau Earth System, National Natural Science
583 Foundation of China (NSFC ERGTPES project No. 42588201), the Department of Science and Technology of
584 the Tibet Autonomous Region (XZ202403ZY0028), and the Second Tibetan Plateau Scientific Expedition and
585 Research Program (2019QZKK0201). AE acknowledges the support from the HINTERLANDS project (High
586 mountains in the Anthropocene: from landscape dynamics to hazards and risks; PRIMUS/25/SCI/005)
587 realized at the Charles University, Faculty of Science; and Johannes Amos Comenius Programme (P JAC),
588 project No. CZ.02.01.01/00/22_008/0004605, Natural and anthropogenic georisks.

590 **Author contributions**

591 Wenfeng Chen and Guoqing Zhang designed the study, and Xue Wang and Wenfeng Chen drafted the
592 manuscript. All authors contributed to the final form of the study.

594 **Data availability**

595 Landsat imagery can be downloaded from the United States Geological Survey (USGS) website
596 (<https://earthexplorer.usgs.gov/>). Sentinel imagery can be downloaded from <https://dataspace.copernicus.eu>.
597 NASADEM data can be downloaded from <https://search.earthdata.nasa.gov>. Glacial lake inventory in 2020 can
598 be downloaded from <https://doi.org/10.6084/m9.figshare.21708590>. The bathymetric measurements for
599 Jialong Co are available at <https://doi.org/10.6084/m9.figshare.21569175>. All process documents including

600 future glacial lake extent, bathymetry, ice thickness and GLOF inventory and simulation outputs are available
601 at <https://zenodo.org/records/16410526>.

602

603 **Code availability**

604 Scripts for the ice thickness inversion model and r.avaflow simulations are available at <https://github.com/cn>
605 [ugis/icethicknessmodel-lake_terminating_galcier](https://github.com/cn/ugis/icethicknessmodel-lake_terminating_galcier).

606

607 **References**

608 [1] Dubey S, Sattar A, Gupta V, et al. Transboundary hazard and downstream impact of glacial lakes in Hindu-Kush
609 Karakoram Himalayas. *Sci Total Environ* 2024;914:169758.

610 [2] Allen SK, Rastner P, Arora M, et al. Lake outburst and debris flow disaster at Kedarnath, June 2013:
611 Hydrometeorological triggering and topographic predisposition. *Landslides* 2016;13:1479–1491.

612 [3] Taylor C, Robinson TR, Dunning S, et al. Glacial lake outburst floods threaten millions globally. *Nat Commun*
613 2023;14:487.

614 [4] Zhang G, Carrivick JL, Emmer A, et al. Characteristics and changes of glacial lakes and outburst floods. *Nat Rev
615 Earth Environ* 2024;5:447–462.

616 [5] Sattar A, Cook KL, Rai SK, et al. The Sikkim flood of October 2023: Drivers, causes and impacts of a multihazard
617 cascade. *Science* 2025;387:eads2659.

618 [6] Zemp M, Jakob L, Dussaillant I, et al. Community estimate of global glacier mass changes from 2000 to 2023.
619 *Nature* 2025;639:382–388.

620 [7] Shugar DH, Burr A, Haritashya UK, et al. Rapid worldwide growth of glacial lakes since 1990. *Nat Clim Chang*
621 2020;10:939–945.

622 [8] Zhang T, Wang W, An B. Heterogeneous changes in global glacial lakes under coupled climate warming and
623 glacier thinning. *Commun Earth Environ* 2024;5:374.

624 [9] Zhang T, Wang W, An B, et al. Enhanced glacial lake activity threatens numerous communities and
625 infrastructure in the Third Pole. *Nat Commun* 2023;14:8250.

626 [10] Carrivick JL, Tweed FS. A global assessment of the societal impacts of glacier outburst floods. *Global Planet
627 Change* 2016;144:1–16.

628 [11] Veh G, Korup O, Von Specht S, et al. Unchanged frequency of moraine-dammed glacial lake outburst floods
629 in the Himalaya. *Nat Clim Chang* 2019;9:379–383.

630 [12] Rick B, McGrath D, McCoy SW, et al. Unchanged frequency and decreasing magnitude of outbursts from ice-
631 dammed lakes in Alaska. *Nat Commun* 2023;14:6138.

632 [13] Veh G, Wang BG, Zirzow A, et al. Progressively smaller glacier lake outburst floods despite worldwide growth
633 in lake area. *Nat Water* 2025;3:271–283.

634 [14] Emmer A. Understanding the risk of glacial lake outburst floods in the twenty-first century. *Nat Water*
635 2024;2:608–610.

636 [15] Zheng G, Allen S, Bao A, et al. Increasing risk of glacial lake outburst floods from future Third Pole
637 deglaciation. *Nat Clim Change* 2021;11:411–417.

638 [16] Shrestha B, Mool PK, Bajracharya SR. Impact of climate change on Himalayan glaciers and glacial lakes: Case
639 studies on GLOF and associated hazards in Nepal and Bhutan. International Centre for Integrated Mountain
640 Development (ICIMOD), 2007.

641 [17] Shrestha BB, Nakagawa H, Kawaike K, et al. Glacial hazards in the Rolwaling valley of Nepal and numerical
642 approach to predict potential outburst flood from glacial lake. *Landslides* 2013;10:299–313.

643 [18] Wang W, Zhang T, Yao T, et al. Monitoring and early warning system of Cirenmaco glacial lake in the central
644 Himalayas. *Int J Disaster Risk Reduct* 2022;73:102914.

645 [19] Niggli L, Allen S, Frey H, et al. GLOF risk management experiences and options: A global overview. Oxford
646 Research Encyclopedia of Natural Hazard Science; 2024.

647 [20] Ding Y, Gong C. Can intergovernmental cooperative policies promote water ecology improvement—An
648 analysis based on water quality data from China's general environmental monitoring station. *PLOS ONE*
649 2023;18:e0294951.

650 [21] Lützow N, Veh G, Korup O. A global database of historic glacier lake outburst floods. *Earth Syst Sci Data*
651 2023;15:2983–3000.

652 [22] Zheng G, Bao A, Allen S, et al. Numerous unreported glacial lake outburst floods in the Third Pole revealed
653 by high-resolution satellite data and geomorphological evidence. *Sci Bull* 2021;66:1270–1273.

654 [23] Shrestha F, Steiner JF, Shrestha R, et al. A comprehensive and version-controlled database of glacial lake
655 outburst floods in High Mountain Asia. *Earth Syst Sci Data* 2023;15:3941–3961.

656 [24] Komori J, Koike T, Yamanokuchi T, et al. Glacial lake outburst events in the Bhutan Himalayas. *Glob Environ*
657 *Res* 2012;16:59–70.

658 [25] Nie Y, Liu Q, Wang J, et al. An inventory of historical glacial lake outburst floods in the Himalayas based on
659 remote sensing observations and geomorphological analysis. *Geomorphology* 2018;308:91–106.

660 [26] Veh G, Lützow N, Kharlamova V, et al. Trends, breaks, and biases in the frequency of reported glacier lake
661 outburst floods. *Earth's Future* 2022;10:e2021EF002426.

662 [27] Allen SK, Sattar A, King O, et al. Glacial lake outburst flood hazard under current and future conditions: worst-
663 case scenarios in a transboundary Himalayan basin. *Nat Hazards Earth Syst Sci* 2022;22:3765–3785.

664 [28] Mergili M, Fischer JT, Krenn J, et al. r.avaflow v1, an advanced open-source computational framework for
665 the propagation and interaction of two-phase mass flows. *Geosci Model Dev* 2017;10:553–569.

666 [29] Mergili M, Emmer A, Juricova A, et al. How well can we simulate complex hydro-geomorphic process chains?
667 The 2012 multi-lake outburst flood in the Santa Cruz Valley (Cordillera Blanca, Peru). *Earth Surf Process Landf*
668 2018;43:1373–1389.

669 [30] Mergili M, Frank B, Fischer J-T, et al. Computational experiments on the 1962 and 1970 landslide events at
670 Huascarán (Peru) with r.avaflow: Lessons learned for predictive mass flow simulations. *Geomorphology*
671 2018;322:15–28.

672 [31] Farinotti D, Huss M, Fürst JJ, et al. A consensus estimate for the ice thickness distribution of all glaciers on
673 Earth. *Nat Geosci* 2019;12:168–173.

674 [32] Zhang G, Bolch T, Yao T, et al. Underestimated mass loss from lake-terminating glaciers in the greater
675 Himalaya. *Nat Geosci* 2023;16:333–338.

676 [33] Sattar A, Allen S, Mergili M, et al. Modeling potential glacial lake outburst flood process Chains and effects
677 from Artificial lake-level lowering at Gepang Gath Lake, Indian Himalaya. *J Geophys Res Earth Surf*
678 2023;128:e2022JF006826.

679 [34] Walder JS, OConnor JE. Methods for predicting peak discharge of floods caused by failure of natural and
680 constructed earthen dams. *Water Resour Res* 1997;33:2337–2348.

681 [35] Westoby MJ, Glasser NF, Brasington J, et al. Modelling outburst floods from moraine-dammed glacial lakes.
682 *Earth-Sci Rev* 2014;134:137–159.

683 [36] Wang WC, Gao Y, Anacona PI, et al. Integrated hazard assessment of Cirenmaco glacial lake in Zhangzangbo
684 valley, Central Himalayas. *Geomorphology* 2018;306:292–305.

685 [37] Anacona PI, Mackintosh A, Norton K. Reconstruction of a glacial lake outburst flood (GLOF) in the Engano
686 Valley, Chilean Patagonia: Lessons for GLOF risk management. *Sci Total Environ* 2015;527:1–11.

687 [38] Kougkoulos I, Cook SJ, Edwards LA, et al. Modelling glacial lake outburst flood impacts in the Bolivian Andes.
688 *Nat Hazards* 2018;94:1415–1438.

689 [39] Chen W, Yao T, Zhang G, et al. Towards ice-thickness inversion: an evaluation of global digital elevation
690 models (DEMs) in the glacierized Tibetan Plateau. *The Cryosphere* 2022;16:197–218.

691 [40] Maranzoni A, D'Oria M, Rizzo C. Quantitative flood hazard assessment methods: A review. *J Flood Risk
692 Manag* 2023;16:e12855.

693 [41] Rounce DR, Hock R, Maussion F, et al. Global glacier change in the 21st century: Every increase in
694 temperature matters. *Science* 2023;379:78–83.

695 [42] Schwanghart W, Scherler D. Short Communication: TopoToolbox 2 – MATLAB-based software for
696 topographic analysis and modeling in Earth surface sciences. *Earth Surf Dyn* 2014;2:1–7.

697 [43] Linsbauer A, Paul F, Hoelzle M, et al. The Swiss Alps without glaciers – a GIS-based modelling approach for
698 reconstruction of glacier beds. *Proceedings of Geomorphometry* 2009; 243–247.

699 [44] Huss M, Farinotti D. Distributed ice thickness and volume of all glaciers around the globe. *J Geophys Res
700 Earth Surf* 2012;117:e2012JF002523.

701 [45] Farinotti D, Huss M, Bauder A, et al. A method to estimate the ice volume and ice-thickness distribution of
702 alpine glaciers. *J Glacio* 2009;55:191, 422–430.

703 [46] Miles E, McCarthy M, Dehecq A, et al. Health and sustainability of glaciers in High Mountain Asia. *Nat
704 Commun* 2021;12:2868.

705 [47] Shean DE, Bhushan S, Montesano P, et al. A systematic, regional assessment of High Mountain Asia glacier
706 mass balance. *Front Earth Sci* 2020;7:363.

707 [48] Frey H, Machguth H, Huss M, et al. Estimating the volume of glaciers in the Himalayan-Karakoram region
708 using different methods. *Cryosphere* 2014;8:2313–2333.

709 [49] Peng M, Wang X, Zhang G, et al. Cascading hazards from two recent glacial lake outburst floods in the
710 Nyainqntanglha range, Tibetan Plateau. *J Hydrol* 2023;626:130155.

711 [50] Niggli L, Frey H, Allen S, et al. Modelling the effectiveness of GLOF DRM measures - a case study from the
712 Ala-Archa valley, Kyrgyz Republic. *EGUsphere* 2025;2025:1–24.

713 [51] Farinotti D, Round V, Huss M, et al. Large hydropower and water-storage potential in future glacier-free
714 basins. *Nature* 2019;575:341–344.

715 [52] Millan R, Mouginot J, Rabatel A, et al. Ice velocity and thickness of the world's glaciers. *Nat Geosci*
716 2022;15:124–129.

717 [53] Steffen T, Huss M, Estermann R, et al. Volume, evolution, and sedimentation of future glacier lakes in
718 Switzerland over the 21st century. *Earth Surf Dyn* 2022;10:723–741.

719 [54] Mölg N, Huggel C, Herold T, et al. Inventory and evolution of glacial lakes since the Little Ice Age: Lessons
720 from the case of Switzerland. *Earth Surf Process Landf* 2021;46:2551–2564.

721 [55] Rinzin S, Dunning S, Carr RJ, et al. Exploring implications of input parameter uncertainties in glacial lake
722 outburst flood (GLOF) modelling results using the modelling code r.avaflow. *Nat Hazards Earth Syst Sci*
723 2025;25:1841–1864.

724 [56] Chen N, Liu M, Allen S, et al. Small outbursts into big disasters: Earthquakes exacerbate climate-driven
725 cascade processes of the glacial lakes failure in the Himalayas. *Geomorphology* 2023;422:108539.

726 [57] Cook KL, Andermann C, Gimbert F, et al. Glacial lake outburst floods as drivers of fluvial erosion in the
727 Himalaya. *Science* 2018;362:53–57.

728 [58] Emmer A, Le Roy M, Sattar A, et al. Glacier retreat and associated processes since the Last Glacial Maximum
729 in the Lejamayu valley, Peruvian Andes. *J S Am Earth Sci* 2021;109:103254.

730 [59] Samui S, Sethi N. Social vulnerability assessment of glacial lake outburst flood in a Northeastern state in

731 India. Int J Disaster Risk Reduct 2022;74:102907.

732 [60] Khadka N, Chen X, Liu W, et al. Glacial lake outburst floods threaten China-Nepal connectivity: Synergistic
733 study of remote sensing, GIS and hydrodynamic modeling with regional implications. Sci Total Environ
734 2024;948:174701.

735

736